Advanced Composite Materials
Publication details, including instructions for authors and subscription information:
http://www.tandfonline.com/loi/tacm20

Influence of residual stresses on the mechanical behavior of composite laminate materials

O. Sicot , X. L. Gong , A. Cherouat & J. Lu

Version of record first published: 02 Apr 2012.

To cite this article: O. Sicot , X. L. Gong , A. Cherouat & J. Lu (2005): Influence of residual stresses on the mechanical behavior of composite laminate materials, Advanced Composite Materials, 14:4, 319-342

To link to this article: http://dx.doi.org/10.1163/156855105774470393

Adv. Composite Mater., Vol. 14, No. 4, pp. 319–342 (2005)

Also available online - www.vsppub.com

Influence of residual stresses on the mechanical behavior of composite laminate materials

O. SICOT *, X. L. GONG, A. CHEROUAT and J. LU

Laboratory of Mechanical Systems and Concurrent Engineering LASMIS (CNRS-FRE 2719), University of Technology of Troyes, 12, rue Marie Curie, B.P. 2060, 10010 Troyes, France

Received 21 January 2005; accepted 28 March 2005

Abstract—Residual stresses occur during most manufacturing processes (from shrinkage of the resin, difference of thermal expansion coefficients, etc.). Residual stresses may cause local yielding and damage initiation and propagation, and can severely affect performances of a composite structure component. The aim of this work is to investigate the influence of residual stresses on the mechanical behavior of carbon/epoxy cross-ply laminates under tensile and torsion loading. The residual stresses field was determined using the incremental blind-hole drilling technique combined with the finite element analysis. The effect of various cure cycles on the residual stress level is analysed. The quantitative effect of the residual stresses on the mechanical behaviour and the damage initiation and growth is studied by using acoustic emission technique.

Keywords: Mechanical properties; residual stresses; cure cycle; acoustic emission

1. INTRODUCTION

The lifetime of a composite component is usually determined by the interactions between the defects within the component and the external stresses to which it is exposed. These stresses are a combination of those applied in service and those that develop during manufacture and processing — the so-called residual stresses. The magnitude of the residual stresses depends on process conditions as well as material properties, part geometry, and lay-up.

Despite the many studies that have been carried out on the subject during the last thirty years, residual stresses remain an important consideration in relation to laminate composite materials. Unlike metals, in which the introduction of residual stresses is sometimes facilitated by a specific treatment such as shot-peening or rolling [1, 2], the presence of residual stresses in laminated structures does not

*To whom correspondence should be addressed. E-mail: olivier.sicot@utt.fr

seem to carry any advantage. It can also cause the resin to micro-crack or produce delamination of the inter-plies before the application of service loading and reduce the service performance of the structure [3, 4].

In many of the studies, the cure cycle was modified in order to reduce the residual stresses [5–10]. Unfortunately, most of the time these cycles lead to a reduction in the final mechanical properties of the material. Finding the best compromise between the level of residual stresses and the final mechanical properties remains a major problem. An effective method is needed to determine the residual stresses, particularly in balanced and symmetrical laminates. The research reported in this project is based on a global approach to residual stresses, designed to encompass all the different problems involved. We first studied the impact of cure conditions on the level of residual stresses in symmetrical laminates $[0_4/90_4]_s$. The residual stresses introduced by the different cure cycles were determined using the incremental hole drilling technique. Secondly, the influence of residual stresses on the mechanical behavior under tensile and torsion loading was investigated. In order to understand the chronology of damage events, the development of individual damage modes, including matrix cracks, inter-ply delamination and fibre fracture, an acoustic emission technique was used during static tensile and torsion tests and the signal interpretations are given by a schematic classification developed previously. The results of this study show that the general level of the residual stresses changes appreciably with the curing conditions and prove that this method gives a new prospect for the study of the distribution of residual stresses in advanced composite parts.

2. CURE CYCLES

Generally, the residual stresses in composite laminates have two principal origins: chemical and thermal. From a chemical point of view, the process responsible for the residual stresses initiation is the increase in the degree of cure (α) and the volumetric contraction of the matrix (μ). From a thermal point of view, the residual stresses appear because of the difference of the longitudinal and transverse thermal dilatation coefficients of each ply of the laminate (α_l and α_t). Several studies showed that the level of the chemical residual stresses remains weak compared to the 'thermal' residual stresses [6, 7]. In this study, only the thermal residual stresses are taken into account.

For the last twenty years, research on the influence of cure cycles on residual stresses in composite laminates has been prolific [5–13]. Many solutions have been considered to reduce the residual stresses level, namely:

- Addition of post-cure treatment [8].
- Reduction in the cooling rate [9, 10].
- Application of hydrometrical fields to facilitate moisture absorption [11].
- Modification of the isothermal step number [8].

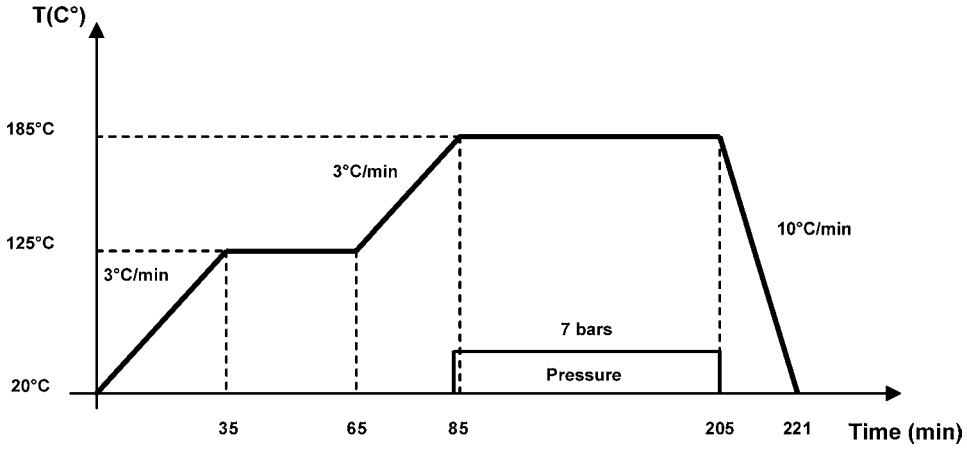

Figure 1. The standard cure cycle.

The aim of this work is not to optimize the cure cycle, but to modify some of its characteristics in order to determine the influence of the residual stresses distribution on the mechanical behavior. To achieve this goal, three types of solutions were proposed: (a) the modification of the cooling rate, (b) the addition of post-cure treatment and (c) the modification of the number of isothermal steps. The reference cycle is a standard two-step cycle (Fig. 1).

Three cure cycles (Fig. 2) are investigated.

- Three cooling rates at a pressure of 7 bars: slow (0.55°C/min), normal or standard (10°C/min) and fast (165°C/min) (Fig. 2a).
- Three temperatures for the additional step introduced during the curing cycle: 150, 160 and 170°C (Fig. 2b).
- Three post-cure treatments at 185°C: 2, 4 and 8 hours (Fig. 2c).

In order to avoid parasitic relaxation of the residual stresses, the post-cure treatments were carried out less than one week after completion of the standard cycle. The post-cure time was intentionally limited so as not to increase too much the total cycle time. Theoretically, it is possible to significantly reduce the residual stresses by applying a relatively long post-cure treatment, but this results in an additional cost which makes the solution expensive. The choice of the additional step temperature for the additional step was established using literature results and considerations relating to the glass transition temperature (T_g) obtained after standard cycle curing (162°C).

To be able to compare the obtained results for the studied cycles, we assessed the degree of cure reached at the end of each cycle. Different measurements carried out showed that the degree of cure is equal to or higher than 0.94. Other authors [5, 6, 14] have shown that beyond 0.91 the evolution of the mechanical characteristics of this type of material is no longer important. In the same way, it

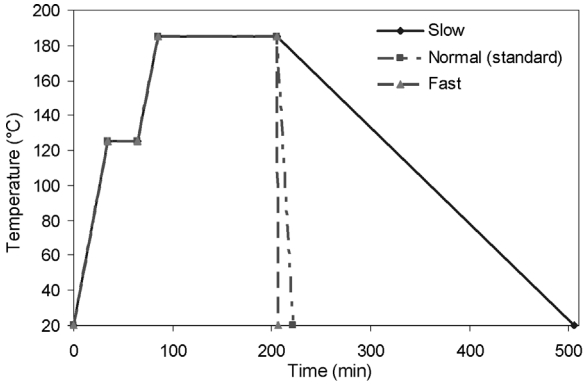

(a) Cooling rate

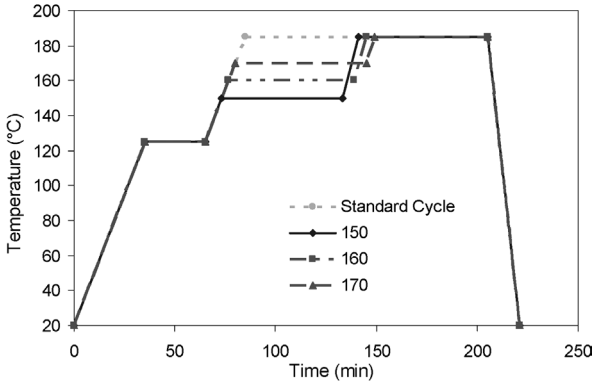

(b) 3 steps

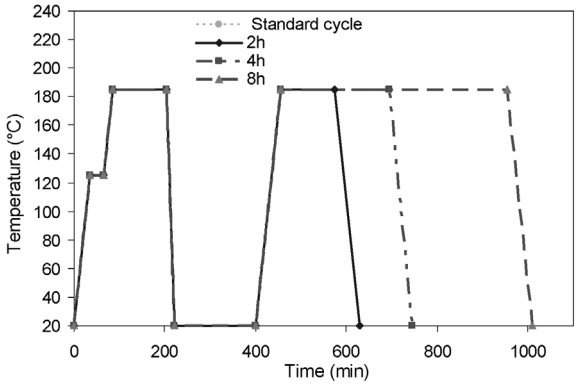

(c) Post cure

Figure 2. The cure cycles used.

appears that the variation of the glass transition temperature is very weak according to the adopted cycles. Thus, we define it as $T_{g\alpha} = 165°\text{C}$.

Also, as the laminate specimens used were relatively thin ($e < 2$ mm), we consider that the temperature is uniform in all the depth of the laminate during the curing cycle (heating and cooling).

The material used as prepreg plies was carbon-epoxy T300/914. The principal characteristics of the resin are: Tensile strength: 57.7 MPa, Tensile modulus: 3.9 GPa, Tensile strain: 1.5%, Poisson ratio: 0.41, T_g: 173°C and Cured density: 1.29 g/cm^3.

The lays-up (using hot press) of the specimens (thickness = 2 mm) were cross-ply $[0_4/90_4]_s$ and unidirectional laminates $[0_{16}]$ and $[90_{16}]$.

3. DETERMINATION OF RESIDUAL STRESSES

3.1. Incremental hole drilling method

Different methods may be used to measure residual stresses in composite structures. The most widely used for non-symmetrical laminates is the observation and measurement of the out-of-plane residual deformation [12, 13]. However, for balanced laminates, only few methods available to measure the evolution of the residual stresses in depth [15, 16].

In a previous study, we developed a new method to measure residual stresses in composite laminates, i.e. the incremental blind hole drilling method [17, 18]. This method can be used to determine the residual stresses profile through the entire thickness of the laminate and in each ply. The principle of the method is based on disturbance of the internal stress field caused by the incremental drilling of a blind hole. The resulting residual strains can be measured using a specific strain gage rosette. The computed calibration coefficients required to calculate the stresses are determined using the finite element method. The composite laminates are modeled by using 3D orthotropic finite elements of ABAQUS/Standard. The numerical method consists in calculating the in-plane surface displacement field produced by incremental hole-drilling. An iterative loading procedure is used to produce numerically the drilling operation. Analysing the increment fields of the displacements and using the Fourier series expansion, we can establish the relationship between the measured surface strains and the corresponding residual stresses through the depth of the material.

The method can be used for all hole drilling configurations and strain gage positions as a result of our development of an automatic calculation procedure for calibration coefficients. With this approach, the redistribution of internal stresses during the drilling of each step is taking into account in the numerical model.

3.2. Results

Figure 3 presents the residual stresses (σ_{xx}), determined using this method for each cure cycles (where 'xx' corresponds to the 0° plies direction). The increments of

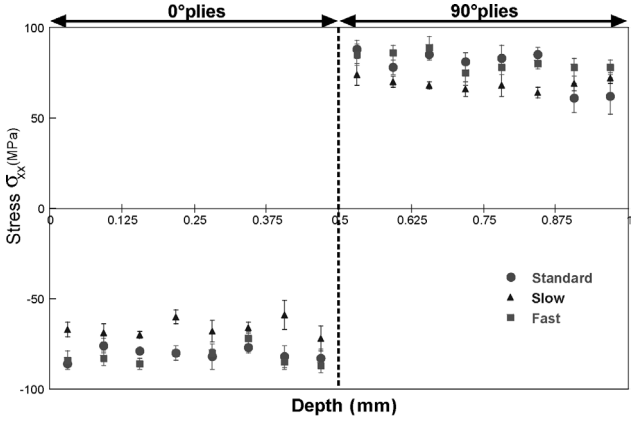

(a) Cooling rate

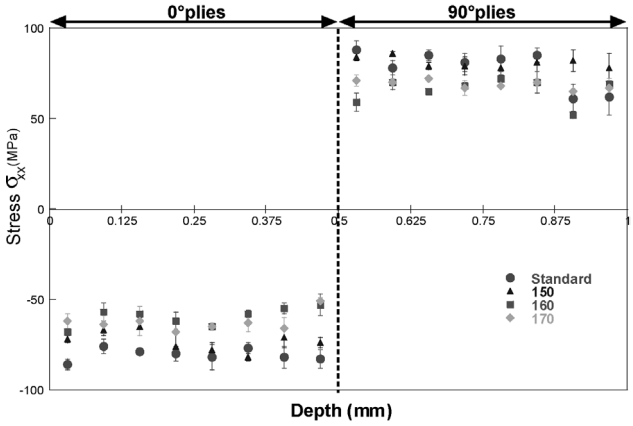

(b) 3 steps

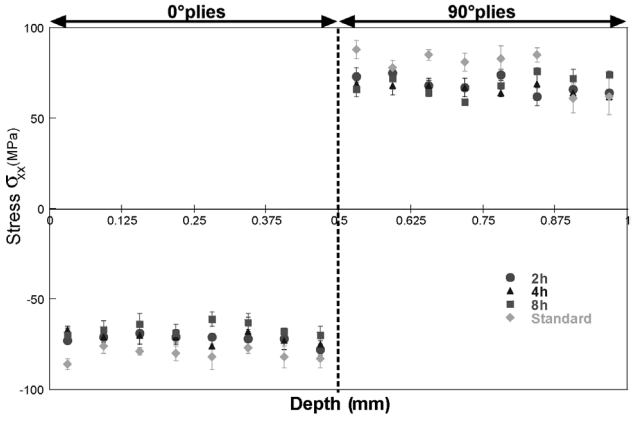

(c) Post cure

Figure 3. Residual stresses (σ_{xx}) for the different cure cycles.

Table 1.
Average of the residual stresses for the plies with the same orientation

		0° plies	90° plies
Cooling rate	Slow	−66	69
	Normal (standard)	−81	78
	Fast	−82	81
Post cure	2 h	−72	70
	4 h	−66	66
	8 h	−65	67
3 steps	150°C	−73	81
	160°C	−59	66
	170°C	−63	69

the drilling have a depth of 62.5 μm, resulting in two increments per each ply. It is therefore possible to predict the stress gradient within each ply. Because of the symmetry of the laminate, the stress profile is only plotted at a depth of 1.0 mm (interface between the 0° and 90° plies is at a depth of 0.5 mm).

In order to compare the measured values obtained for various cycles, Table 1 presents average values of the calculated stresses on the plies with the same fibres orientation.

It may be noted that the same residual stress distribution was obtained for the all tested cure cycles. The 0° plies are under compressive stresses (≈ -70 MPa) while the 90° plies are under tensile stresses. We also noted that the compressive and tensile stresses were symmetrical ($\approx +70$ MPa), which corresponds to the total balance of the residual stresses field for all thicknesses. More specifically, the residual stresses determined seem to be higher at the 0°/90° interface. The results obtained during this study show the effect of the cure cycle condition on variations in the residual stresses.

At the same time, we note that the measured values of residual stresses are higher (+30%) than those generally determined by a thermoviscoelastic approach of the classical theory of the laminate (CLT). Figure 4 presents the profile of residual stresses (σ_{xx}) determined by a thermoviscoelastic approach of the CLT profile for three cure cycle (standard, 3 step cycles (160°C) and post-cure (8 h)).

Three main reasons to explain this difference can be proposed:

– the drilling process introduces damage (such as microcracking or delaminations) which causes a parasitic stresses relaxation,

– the determination of calibration coefficients (Subsection 3.1) is carried out by an elastic and not viscoelastic approach,

– generally, the results obtained by the classical theory of the laminate do not take into account the phenomena of porosity and the stresses of chemical origin.

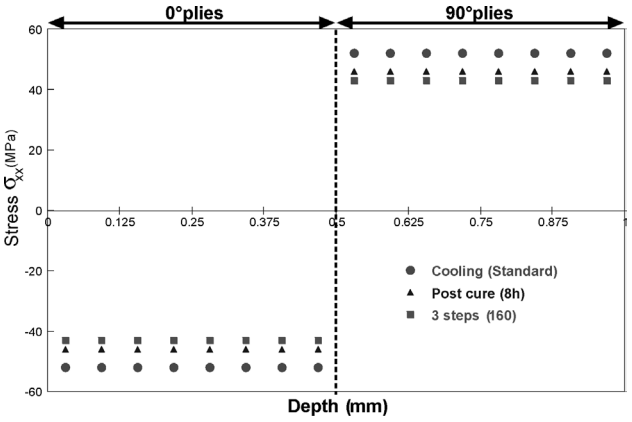

Figure 4. Residual stresses (σ_{xx}) for three cure cycles. Thermoviscoelastic approach of the CLT.

Nevertheless, even if these variations exist, it is possible to analyze the relative influence of the cure cycle on the residual stresses level and then on the mechanical behavior.

3.2.1. Cooling rate. The obtained results (Fig. 3a and Table 1) show the influence of the cooling rate on the residual stresses. We observe that the reduction of the cooling rate leads to a sensible reduction of the residual stresses ($\sigma_{xx} = -66$ MPa for slow cooling, $\sigma_{xx} = -81$ MPa for normal cooling and $\sigma_{xx} = -82$ MPa for fast cooling). These results can be explained by the viscoelastic properties of the resin. Indeed, a slow cooling (here, 0.55°/min) allows, after the second step, an important relaxation of the residual stresses. On the other hand, a fast cooling (>100°/min) does not allow this relaxation. Within the framework of a viscoelastic approach of the classical laminate theory (CLT), the residual stresses level depends directly on the difference between the cure and the room temperature [8, 12]. However, even if the reduction of the cooling rate leads to a significant decrease of the residual stresses ($\approx -20\%$), this solution presents the drawback of appreciably increasing the duration of the cure cycle ($\approx$ 200 min for the normal cooling and 500 min for the slow cooling), which reduces of as much its economic effectiveness.

3.2.2. Three-step cure cycles. The three-step cure cycles were tested in order to mimic the standard cycle with two steps followed by a post-cure cycle. The function of the second step is to make it possible to reach a high level of cure at a relatively low temperature. As for the third stage, it must ensure a complete cure and a reticulation close to unity. The obtained results (see Fig. 3b and Table 1) seem to indicate that the introduction of a third step leads to a reduction of the level of residual stresses. Indeed, for the step at 160°C and 170°C we obtain a significant reduction of the stresses compared to the standard cycle (for σ_{xx}, equal to -59 MPa, -63 MPa and -81 MPa for 160°C, 170°C and the standard cycle, respectively).

With regard to the 150°C step, we observe a decrease of the residual stresses but it is less important ($\approx 10\%$). Probably, the length and the temperature of the step are not sufficiently high to reach a high level of cure. Thus, the end of the cure will take place during the third step.

3.2.3. Post-cure cycles. During the post-cure cycles, two phenomena play an important role. Firstly, the viscoelastic behaviour of the resin can lead to a residual stresses relaxation. Secondly, the post-cure cycle can ensure a complete cure and thus increase the level of residual stresses. In our case, results seem to show that it is the first phenomenon that dominates. Indeed, compared to the standard cycle, we observe a general reduction in the average residual stresses with the introduction of the post-cure ($\sigma_{xx} = -72$ MPa, -66 MPa, -65 MPa and -81 MPa for the post-cure of 2 h, 4 h, 8 h and the standard cycle respectively) (see Fig. 3c and Table 1). After 4 h and 8 h of post-cure, the reduction in residual stresses is reduced to 20%. On the other hand, the reduction in stresses is around 10% for 2 h of post-cure. Thus, after a certain time, the increase of the post-cure duration does not cause any significant reduction of the residual stresses level. However, for standard cure cycle, the reduction in level of stresses is very weak due to the short time post-cure. The results of the mechanical tests will show us if this reduction in residual stresses is accompanied by a deterioration in mechanical properties.

Results give to a certain extent the relative effectiveness of the various cycles to reduce the level of the residual stresses. Thus, it appears that the addition of a sufficiently long post-cure, the reduction of the cooling rate as well as the introduction of a third step can lead to a major reduction of the level of the residual stresses. However, additional time due to the post-cure and the lengthening of the duration of cooling makes these solutions expensive. On the other hand, the introduction of a third step allows an important reduction of the stresses without increasing the duration of the cure cycle and this solution represents the best compromise.

4. MECHANICAL TESTS

The above results show the significant influence of the cure cycles on the level of residual stressesl. To determine the effect of residual stresses on mechanical behavior, two tests are investigated, tension and torsion.

4.1. Tensile tests

The tensile tests have two main objectives:

- To determine whether or not the cure cycles previously presented modify the main mechanical properties of the laminates.
- To highlight the impact of residual stresses on the fracture properties and on damage initiation and propagation.

The tensile tests were carried out on two different tensile machines. The transverse modulus was determined on the $[90_{16}]$ laminates using an Instron 4214 with a capacity of 10 kN. The other tests were carried out on a machine with a capacity of 150 kN (determination of the longitudinal modulus and Poisson's ratio on $[0_{16}]$ laminates and the influence of residual stresses on $[0_4/90_4]_s$ laminates). The tensile speed was fixed at 1 mm/mn.

4.1.1. Acoustic emission technique. Acoustic emission is a non-destructive technique allowing detection and a significant analysis of damage in materials and particularly in composite materials. This technique relies on the exploitation of the elastic wave propagation in materials at ultrasonic frequencies. The origin of these waves is the mechanical vibrations due to the release of energy generated by the application of a mechanical stress field. One of the major advantages of this technique is the possibility of following in real time the damage initiation and its evolution.

Two methods were used to process the acoustic signals, namely, the cumulated counts, which can be used to detect damage initiation [19, 20] and the amplitude treatment used to monitor the development of different types of damage during the test [21, 22]. This treatment relies on the identification of a type of damage with a aprticular amplitude range. In spite of the fact that this method is still controversial, many authors have determined a more or less precise range of amplitudes for each type of damage [23, 24]. In this study, we took as reference the work realized by the team of M. L. Benzeggagh [19, 24]. From specific tests, they established, for laminate carbon/epoxy, the following distribution of amplitude:

- Microcracking of the resin: 34–45 dB.
- Coalescence of the microcracking: 46–58 dB.
- Fracture of the fiber/matrix interface: 59/69 dB.
- Friction fiber/matrix: 70–86 dB.
- Fiber breaking: 87–95 dB.

It should be noted that this distribution of amplitude is not fixed. According to the experimental conditions used, it is possible that these ranges may change. To be able to use the distribution presented above, we adopted strictly the same procedure and the same adjustments described in Refs [21, 22].

Thus, the acoustic activity was recorded and analyzed using a Vallen AMSY4 acoustic emission system. A 39 dB preamplifier was located just after the piezoelectric sensor (SE375-M#212) and fixed to the surface of the test specimen. A second amplification of 40 dB was made to the collected signal. Figure 5 is a schematic representation of the experimental device used for the tests. Figure 6 presents the typical tensile curve for a $[0_4/90_4]_s$ laminate and the associated cumulated acoustic emission curve. Two characteristic points can be observed: damage initiation (significant onset of acoustic activity) and final fracture.

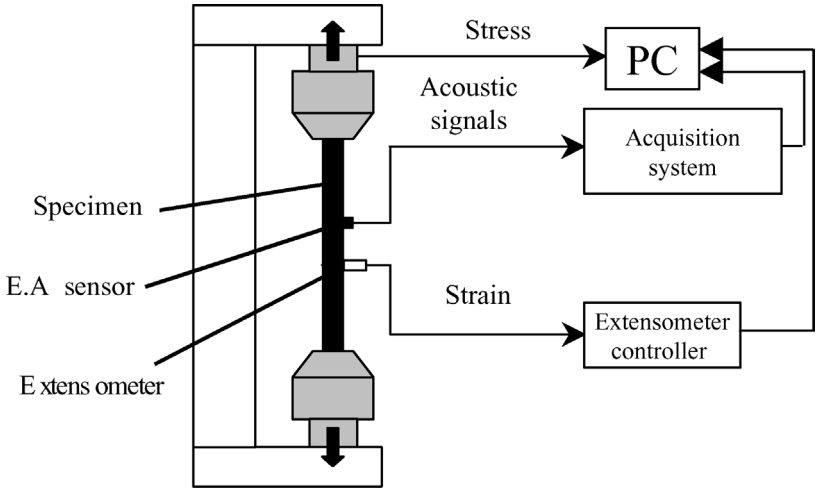

Figure 5. Experimental device for traction tests.

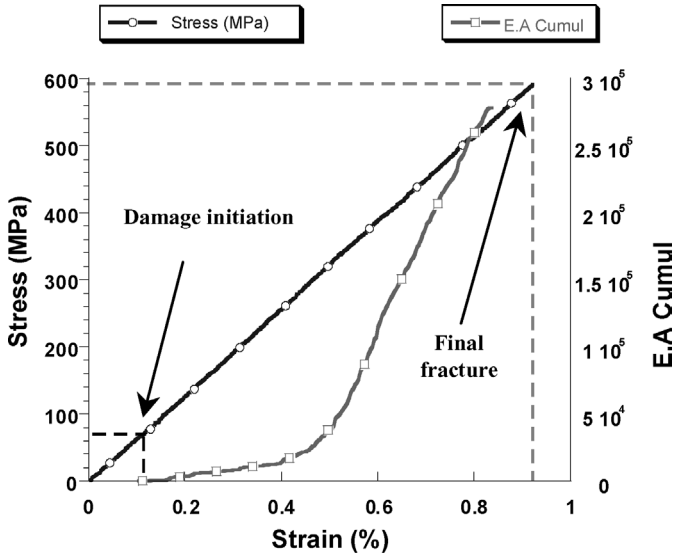

Figure 6. Determination of the two characteristic points on the tension curve. Damage initiation and fracture stresses.

4.1.2. Unidirectional laminates. As mentioned above, we first investigated the influence of the cure cycles on the mechanical behavior of the unidirectional laminates. Figures 7, 8 and 9 show the change in the longitudinal and transverse modulus (E_{11} and E_{22}, respectively) and the in-plane Poisson's ratio ν_{12} for the different cure cycles.

In these figures, we can note that, the increase in the cooling rate leads to a decrease in the E-moduli (7% for E_{11} and 4% for E_{22}) and the increase in the post-cure time leads to an increase in the E-moduli (Figs 7 and 8). After 8 hours of

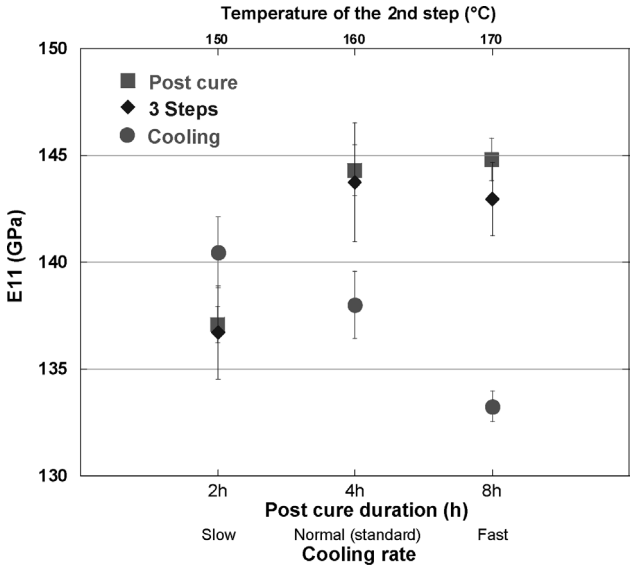

Figure 7. Longitudinal modulus E_{11}.

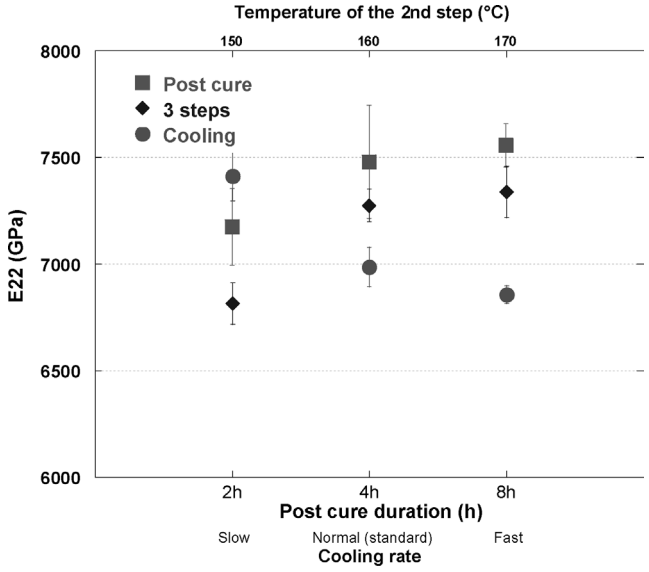

Figure 8. Transverse modulus E_{22}.

post-cure treatment, the longitudinal modulus is $E_{11} = 145$ GPa and the transverse modulus E_{22} is very close to 7500 MPa. The Poisson's ratio is $\nu_{12} = 0.27$. However, the increase in the elastic properties resulting from the post-cure treatment remains limited. The difference observed for the longitudinal modulus is about 6% (between 8 h and 2 h of post cure) while it is 8% for the transverse modulus (between standard cycle and 8 hour post-cure treatment). At same time, we note an increase of 10%

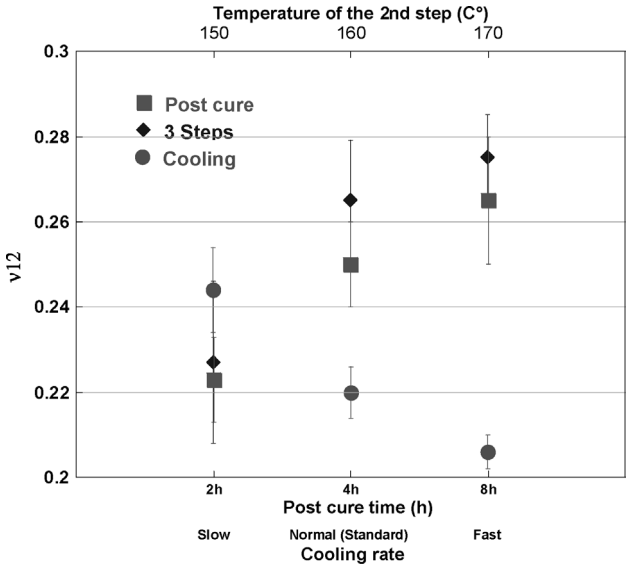

Figure 9. Poisson ratio ν_{12}.

in the Poisson's ratio between the standard cycle (no post-cure treatment), and the 8 hour post-cure treatment (Fig. 8). It was noted that the third step temperature leads to an increase in the elastic properties. For the longitudinal modulus E_{11}, the increase is 6% (between the 160°C and 150°C steps, respectively) while it is 7% for the transverse modulus (between the 170°C and 150°C steps) and the Poisson's ratio. It was also noted that the results obtained for the 160°C and 170°C steps are very similar (the difference is usually less than 2%) and the standard cure cycle (two steps) does not lead to higher elastic properties. It seems that the cycle recommended by the manufacturer is not optimal. With respect to the influence of the cooling rate, the results show that slow cooling increases the modulus and the Poisson's ratio. If fast cooling is used, however, the curing process is not completed.

With respect to the effectiveness of the cure cycle and the results on residual stresses, it appears that the introduction of a third isothermal step is a better solution than the addition of a post-cure treatment or a decrease in the cooling rate.

4.1.3. Cross-ply laminates. For the cross ply laminates, the apparent 'modulus' E_{xx} for each cure cycles is given in Fig. 10. It can be clearly seen that the modulus varies in the same way as it does for unidirectional laminates. Increasing the post-cure time increases the modulus (+7% between the standard cycle and the 8 hours post-cure cycle). However, it can be noted that the results obtained for 4 h and 8 h post-cure are very similar.

The effects of the 3-step cure cycle are almost the same. The 150°C step leads to a slight decrease in the modulus while, in the 160°C and 170°C steps, the increase is 8%. A comparison of the results obtained for the two types of cycles confirms that introducing a third step is equivalent, in terms of mechanical properties, to

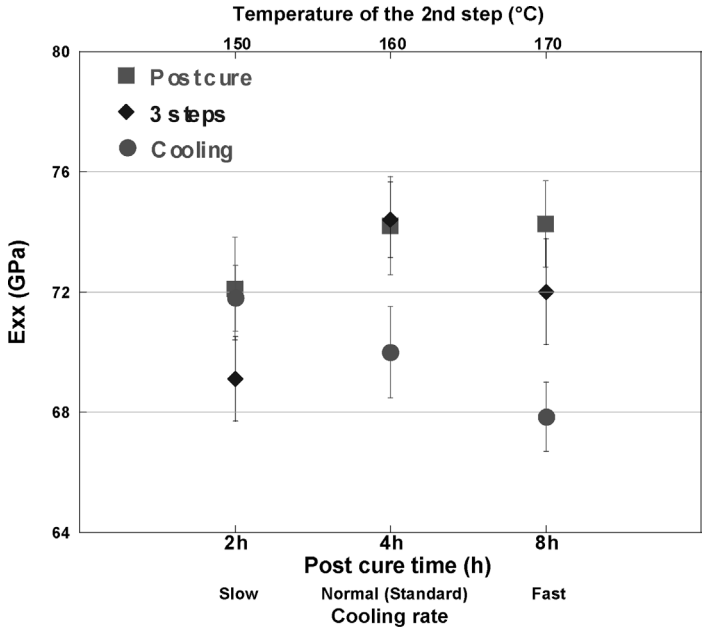

Figure 10. Apparent modulus E_{xx}.

the addition of a 4 or 8 hours post-cure treatment. It would therefore appear that, from an economical viewpoint, the addition of post-cure treatment is not the best economic solution.

The above results show the existing relation between the evolution of the E_{xx} modulus and the level of the residual stresses. Indeed, overall we observe that the lower the residual stresses, the higher is the modulus. To better understand the evolution of this modulus, in addition to the residual stresses effect, we show the role of the degree of cure reached at the end of each cycle. Indeed, the E_{xx} modulus is more important for the cycle with post-cure of 4 h and 8 h than for the cycle with 3 steps (160°C). However, it appears precisely that these cycles lead to a complete cure of the resin. As we have considered previously, for these cycles the completion of the cure process seems also to be accompanied by an important relaxation of the residual stresses. We note the same tendency with regard to the E_{11} modulus and the E_{xx} modulus.

4.1.4. Damage analysis. Figure 11 shows the damage initiation and fracture stresses, determined using the acoustical emission method for different cure cycles.

We can note that the fracture stress is less influenced by the post-cure time (5% difference between 2 h and 8 h). However, the damage initiation is largely dependent on the post-cure time. Between 2 h and 8 h, the difference is about 20% (between 42 MPa and 53 MPa). If the standard cycle is considered, it can be seen that the damage initiation stress varies almost linearly with the post-cure time. The damage initiation stress directly depends on the temperature of this step

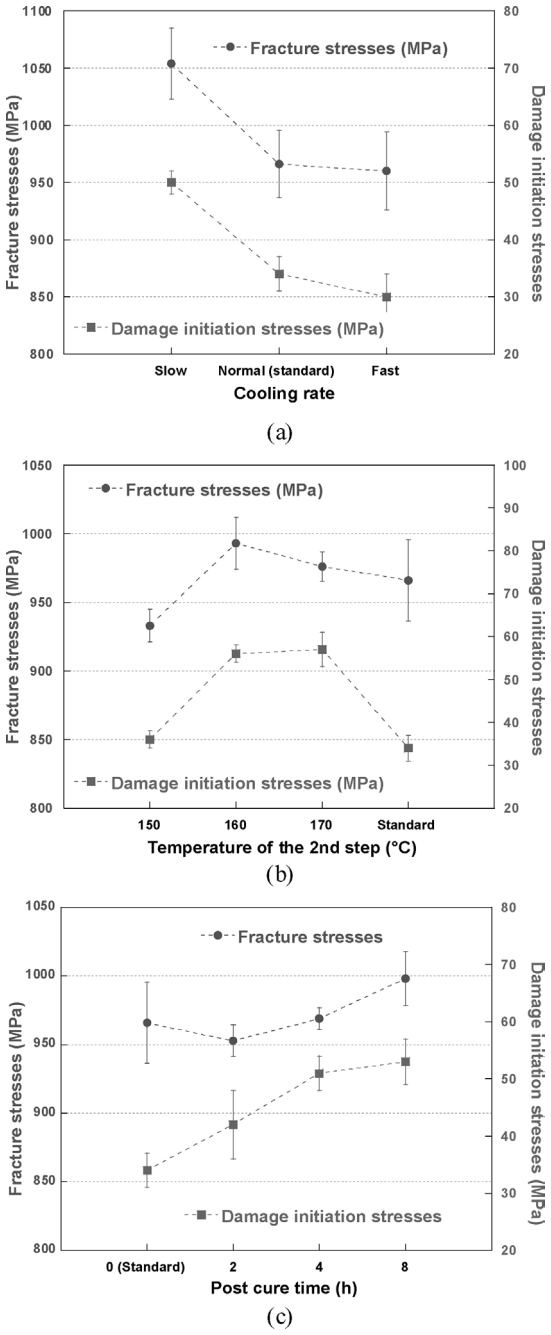

Figure 11. Damage initiation and fracture stresses.

(30% between 150°C and 160°C) while the fracture stress increases only slightly (6% between 150°C and 160°C). From our analysis of the relationship between the

level of residual stresses and unidirectional laminates, a certain dichotomy can be noted between the 160°C and 170°C steps on one hand, and the 150°C step and the standard cycle on the other hand.

In order to illustrate the relationship between the residual stress level and the mechanical properties, all the tests showing the average damage initiation stresses

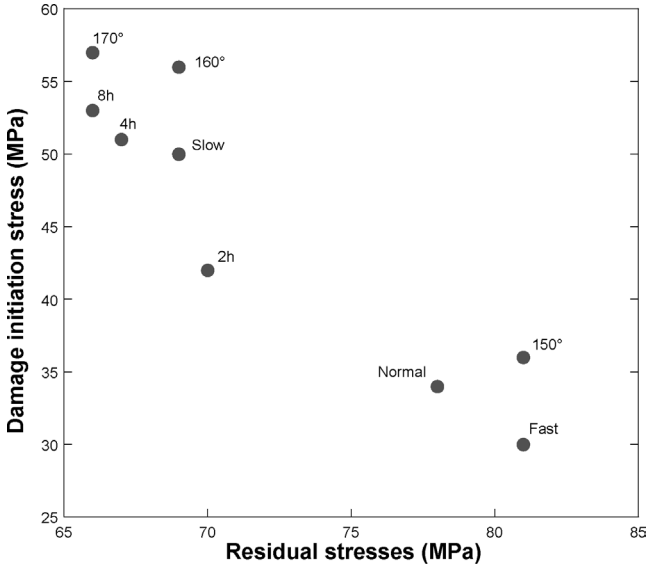

Figure 12. Damage initiation stress in function of residual stresses (90° plies).

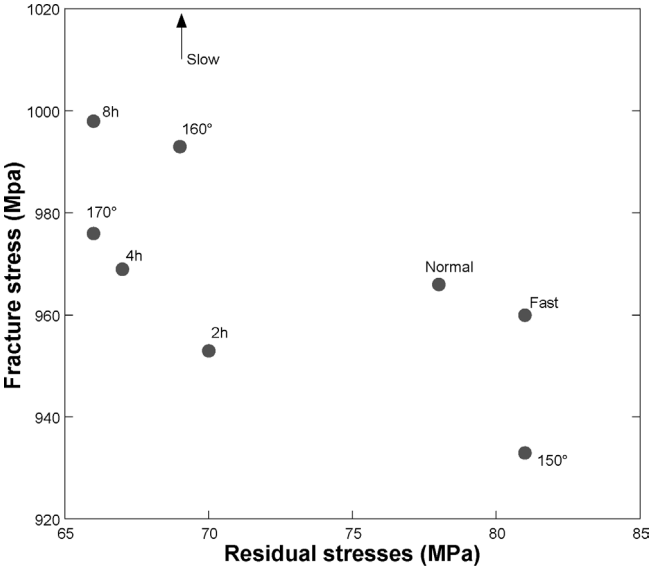

Figure 13. Fracture stress in function of residual stresses (0° plies).

and residual stresses in 90° plies are presented in Fig. 12. It seemed judicious to choose the residual stresses in the 90° plies for comparative data because with a $[0_4/90_4]_s$ laminate, the damage in uniaxial traction in the longitudinal direction appears initially as transverse microcracking in these plies. This figure particularly highlights the influence of the residual stresses on the damage initiation stresses. It appears that a high level of residual stresses accelerates damage initiation.

For the fracture stresses, we used the average level of the stresses in the 0° plies. Indeed, although the final fracture is dependent on the complete history of the laminate, in particular of the successive fracture of the 90° plies, the final fracture of the specimen occurs after the fracture of the 0° plies (Fig. 13).

The influence of the residual stresses on the fracture stresses can be detected, but it seems less significant than its effect on the damage initiation stress (Fig. 12).

Figure 14 presents the amplitude distribution of cumulative AE events for four different stresses levels in 8 hours post-cure cycle.

Some remarks are appropriate:

- At 40 MPa (Fig. 14a), damage initiation has not yet taken place. A few low amplitude signals can be noted (probably noise due to the contact between sensor and sample).

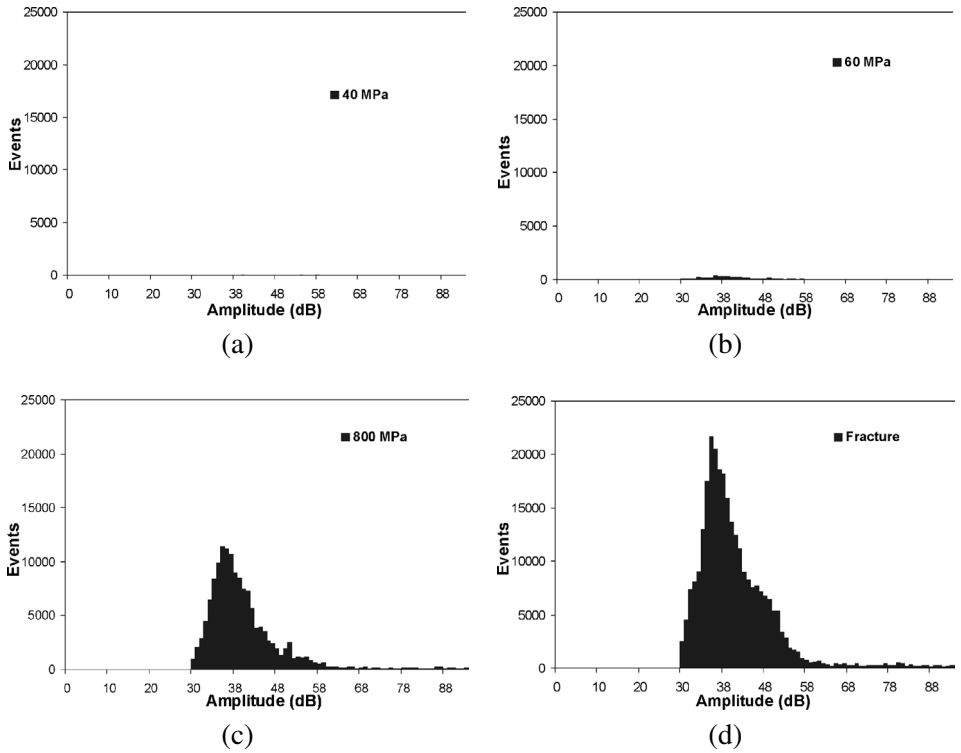

Figure 14. Amplitude treatment (8 hours post-cure cycle). Cumulative AE events.

- At 60 MPa (Fig. 14b), damage initiation takes place. The onset of signals in the vicinity of 40 dB can be noted. According to the classification adopted [21], these signals correspond to microcracking of the resin in the 90° plies.
- At 800 MPa (Fig. 14c), the laminate is much damaged. An appreciable increase in signals can be observed. Their distribution is slightly directed towards higher amplitudes. Many signals were detected with amplitude of 50 dB to 60 dB. According to the same schematic classification, these amplitudes correspond to the coalescence of microcracks. The appearance of signals with higher amplitudes was also noted, but in relatively small numbers.
- When fracture takes place (at 1000 MPa see Fig. 14d), the distribution of signals is appreciably similar to that recorded at 800 MPa. Most of the signals are in the 35 dB to 45 dB range. However, signals with high amplitudes (>70 dB) may correspond to fiber/matrix friction and the fiber fracture.

We applied the same process to all the tests included in the study. Generally speaking, both the initiation and type of damage are the same for all the tests. Nonetheless, a small difference was observed which is potentially due to the presence of residual stresses. In particular, it was noted that acoustic activity was appreciably less when the post-cure time was increased. The same phenomenon occurred when the temperature of the second step increased. To illustrate this and for each amplitude we calculated, the difference (D) in the number of signals between the 2 h and 8 h post-cure cycles, as follows:

$$\mathrm{D} = \mathrm{N}_i(8\ \mathrm{h}) - \mathrm{N}_i(2\ \mathrm{h}) \quad \text{with } i = 30, \ldots, 100\ \mathrm{dB}, \tag{1}$$

where N_i is the number of signals for each amplitude (5 MPa before final fracture) (Fig. 15).

This result highlights an important gap in the 40 to 60 dB amplitude range, which largely corresponds to the coalescence of microcracks. One explanation for the

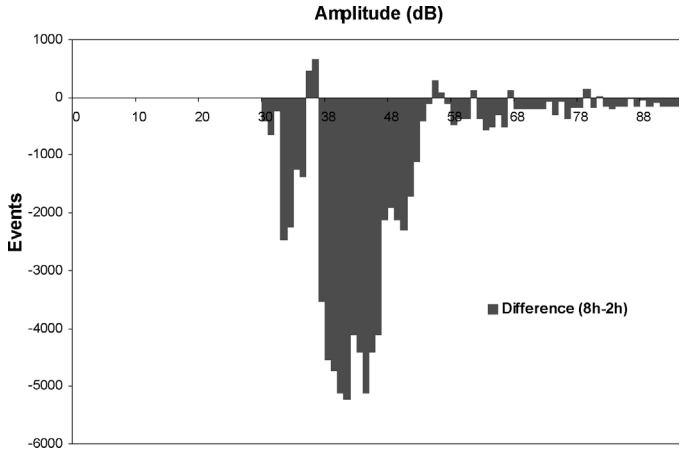

Figure 15. Comparison of the acoustic activity for different cycles (8 h–2 h).

lack of signals could be the presence of residual stresses. The higher the residual stresses, the earlier damage initiation will occur. Thus, for the same service loading, a laminate structure with a high residual stresses field will sustain greater damage, resulting in higher acoustic activity.

4.2. Torsion test

In order to continue to investigate the influence of residual stresses on the mechanical behavior, torsion tests were carried out. These tests were performed because we wanted to study the influence of the residual stresses when combined loads as tension/torsion, flexion/torsion were applied. However, before applying these types of load, it is essential to understand what occurs for each simple situation, and to consider the mechanics or acoustics. Finally, these tests must also inform us about the validity of one of the assumptions used within the hole-drilling method. Indeed, by assumption, for the various calculations of residual stresses we neglect the shear stress component τ_{xy}. With this approach we determine only one biaxial stress field (σ_{xx} and σ_{yy}). However, for torsion tests, the shear stress component plays the most important part. Therefore, following these tests, it will be possible for us to determine if this initial assumption is valid.

The same experimental set-up was adopted as that used for the tensile tests. The damage initiation torque was determined for each cycle studied while the fracture torsion was obtained by acoustic emission. All the tests were performed using a Torsiomat C10 machine with a maximum applied torsion of 12 N m. The angular velocity was fixed at 0.5°/mn. The dimensions of the used specimens $[0_4/90_4]_s$ were $140 \times 15 \times 2$ mm.

To monitor the damage, we had to restrict the field of investigation. Unlike the tensile tests, the acoustic sensor is not always in contact with the surface of the test specimen during the torsion tests. For this reason we limited our study of the damage to an angle of 80°. However, the torsion tests were performed up to until fracture of the test specimens. Figure 16 illustrates the torque damage initiation and fracture for different cure cycles conditions (cooling rate, post cure time and 3-step).

The figures show the influence of the cure cycles conditions, and therefore the residual stresses, on the composite shear properties. In first analysis, the results show that the curing conditions influence is less important in torsion than in traction. For all conditions, the fracture angles vary between 195° and 215° while the torsion moment ranges from 6.32 N m to 6.54 N m. For example, for the slow cooling condition, the torque damage initiation is for 0.55 N m and the torque fracture is 6.43 N m (Fig. 16a). For the post-cure cycle (Fig. 16b) and the 3-step cure cycle (Fig. 16c), a relative dichotomy, similar to that observed during the tensile tests, is observed between the 160°C and the 170°C cycles, on the one hand (respectively, 6.49 N m and 6.51 N m for the fracture torque), and the standard and the 150°C cycles on the other hand (6.27 N m and 6.34 N m for the fracture torque, respectively). The same results for normal and fast cooling were also observed while they were slightly higher for slow cooling (Fig. 16a). With regard to the damage

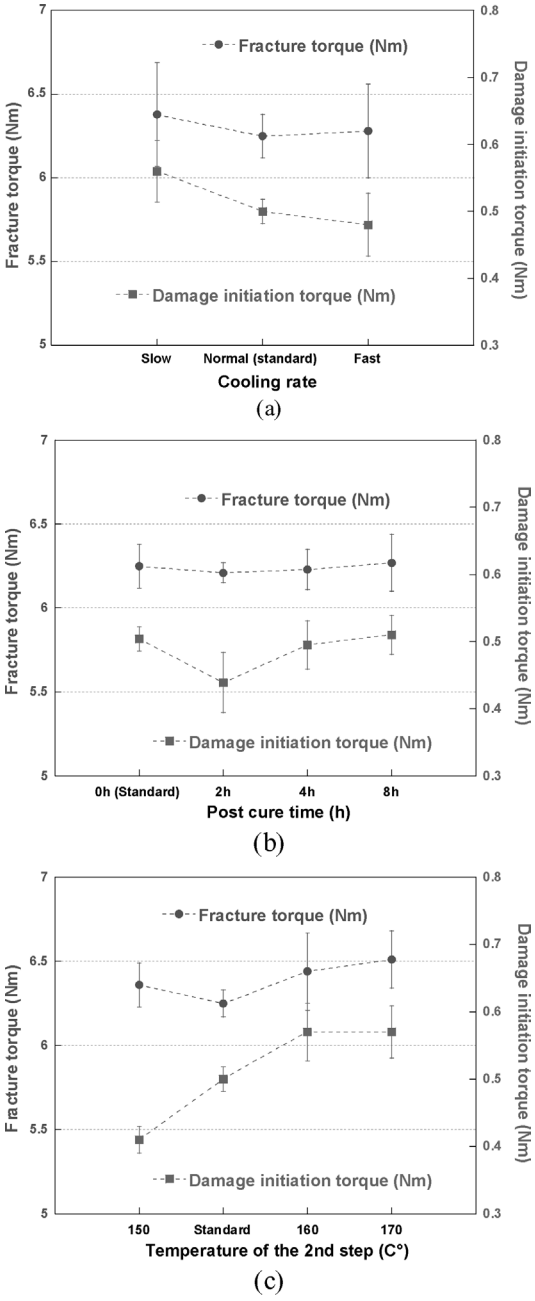

Figure 16. Damage initiation and fracture torsion.

initiation characteristics, approximately the same tendency was noted for both the damage initiation and the fracture characteristics.

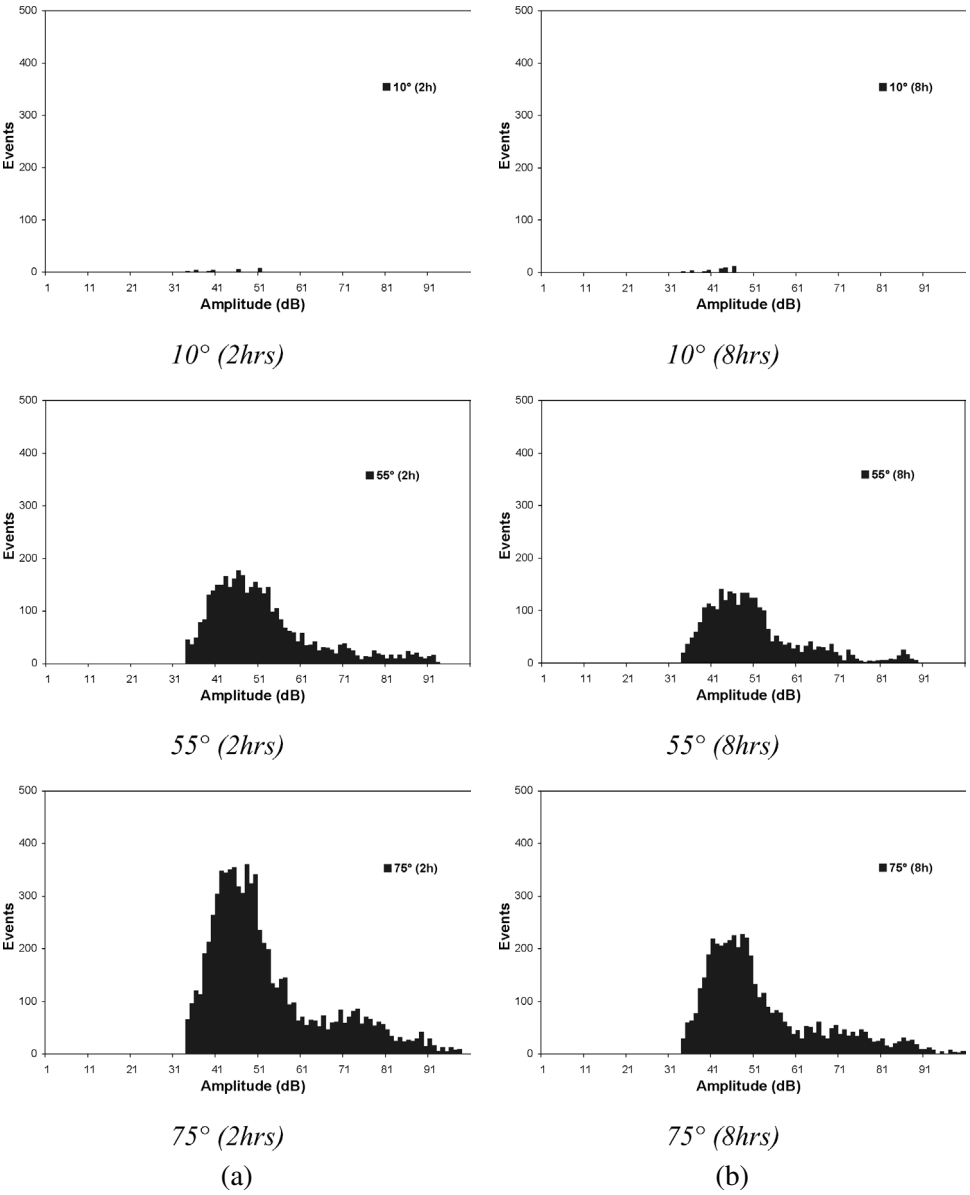

Figure 17. Comparison of acoustic activity (amplitude treatment). (a) 2 hours post cure cycle, (b) 8 hours post cure cycle.

Figure 17 presents the amplitude distribution of cumulative AE events observed for the 2 h and 8 h post-cure cycle at three different torque loadings (10°, 55° and 75°). The AE distributions are representative of the all obtained results.

They also allow us to establish qualitative and quantitative comparisons with those obtained with tensile tests:

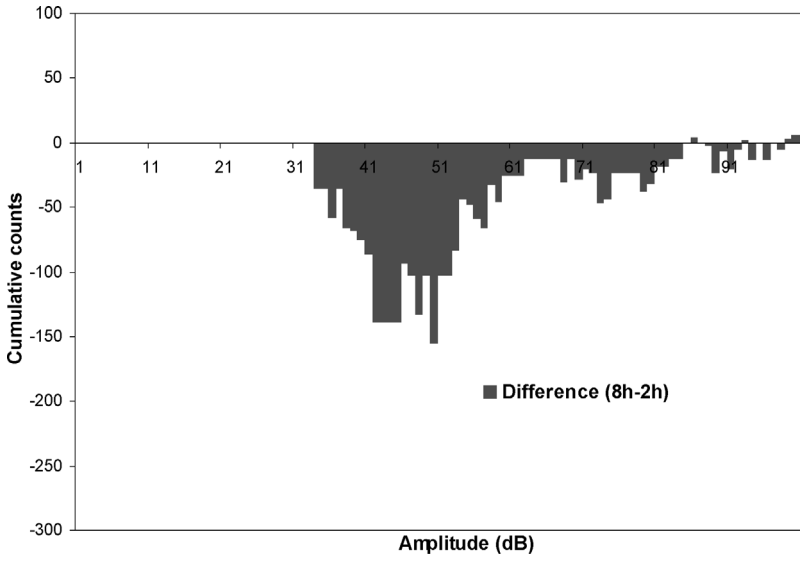

Figure 18. Comparison of acoustic activity for different cycles (8 h–2 h). Torsion test.

- Qualitatively: It was noted that the peak signals were in the vicinity of 45 dB, which was also observed in the tensile tests. The amplitude distributions are characterized by the onset of a peak signal of about 75 dB. According to the schematic classification adopted, this amplitude corresponds to the fiber/matrix fracture interface and fiber/matrix friction. Therefore, although micro-cracking of the resin is still the most important damage process, it seems that another process appears relatively early in the procedure.
- Quantitatively: Up to a rotation of 20°, the damage is only very slight. After that, significant damage occurs. The onset of a signal peak at the vicinity of 45 dB was observed. For rotation of 55°, the number of signals with amplitude of 60 dB to 90 dB is significant. Between 55° and 75°, the damage developed dramatically and a peak of 75 dB was clearly observed.

With the same type of treatment applied to all the torsion tests, we find approximately the same conclusions as that during the tensile tests. Indeed, whatever the level of residual stresses within the laminate, we observe essentially the same evolution of the acoustic activity for all the tests. Thus, the first acoustic signals are always centered on 45 dB. Then, we note a rapid increase in the number of signals and finally we observe the onset of a second acoustic peak centered on 75 dB. With regard to the relative acoustic activity between all cure cycles, we note the same tendency as in tension. In fact, for example, the acoustic activity is appreciably less when the post-cure time increases and when the temperature of the second step increases. As in the tension case, Fig. 18 presents the difference of acoustic activity (D) between the 2 h and 8 h post-cure cycles (at 75° of rotation).

This figure shows the increase in the acoustic activity with the post-cure decrease. However, in a general way, it is noted that the differences in acoustic activity are less important in torsion than in tension. Indeed, even if both tests are not directly comparable because the recording of the acoustic activity in torsion was not carried out until the fracture of the specimens, we note from Figs 15 and 18 that the difference in cumulative events for each amplitude is appreciably less important in torsion than in tension. This difference reaches '5000' events for tension whereas it reaches '150' for torsion.

At the same time, the analysis of the amplitude distribution shows that the acoustic activity profile for the torsion tests differs from that of the tensile tests. During the torsion tests, fiber/matrix interface fracture and fiber/matrix friction appeared early. The premature initiation of this type of damage is more accentuated when the residual stress level is important.

5. CONCLUSION

The influence of the cure cycle on the residual stress level has been investigated in this study. The introduction of a third isothermal step and the addition of post-cure treatment at the end of the standard cure cycle appreciably reduced the level of residual stresses. However, the 3-step cure solution appears to be a better solution than post-cure treatment.

The second part of the study highlighted the influence of residual stresses on mechanical behavior under tensile and torsion loading. The results obtained for unidirectional laminates showed that changing the cure cycle has very little effect on the longitudinal and transverse modulus and the in-plane Poisson coefficient. The cross-ply laminate tests $[0_4/90_4]_s$ showed that the apparent modulus is not modified to any significant degree by the presence of residual stresses. The acoustic emission technique was used to study damage initiation and monitor damage development during testing.

It has been clearly shown that a high level of residual stresses accelerates damage initiation and growth. The same type of influence was observed on the fracture characteristics, although less significant. The amplitude analysis allowed us to identify the different damage processes which occurred during both tests. It showed a significant rise in acoustic activity with an increase in residual stresses.

REFERENCES

1. S. Tekeli, Enhancement of fatigue strength of SAE 9245 steel by shot-peening, *Mater. Letters* **57**, 604–608 (2002).
2. D. Retraint, C. Garnier, *et al.*, Improvement of fatigue behaviour of an automotive part using a new mechanical treatment, *Mater. Sci. Forum* **404–407**, 463–468 (2002).
3. D. Perrreux and D. Lazuardi, The effect of residual stresses on the non-linear behaviour of composite laminates, Part I. Experimental results and residual-stresses assessment, *Compos. Sci. Technol.* **61**, 177–190 (2000).

4. R. G. Spain, Thermal microcracking of carbon fibre/resin composites, *Composites* **2**, 289–298 (1971).
5. S. R. White and H. T. Hahn, Mechanical properties and residual stresses development during cure of a graphite/BMI composite, *Polymer. Eng. Sci.* **30**, 1465–1473 (1990).
6. S. R. White and H. T. Hahn, Process modeling of composite materials: residual stresses development during cure, Part II. Experimental validation, *J. Compos. Mater.* **26**, 2423–2451 (1992).
7. H.-B. Wang, Y.-G. Yang, *et al*., Assessment of residual stresses during cure and cooling of epoxy resins, *Polym. Eng. Sci.* **35**, 1895–1898 (1995).
8. S. R. White and H. T. Hahn, Cure cycle optimization for the reduction of processing-induced residual stresses in composite materials, *J. Compos. Mater.* **27**, 1352–1377 (1993).
9. Y. Weitsman, Residual thermal stresses due to cool-down of epoxy-resin composites, *J. Appl. Mech.* **46**, 563–567 (1979).
10. W. J. Unger and J. S. Hansen, The effect of cooling rate and annealing on residual stresses development in graphite fibre reinforced PEEK laminates, *J. Compos. Mater.* **27**, 108–137 (1993).
11. D. A. Douglas and Y. Weitsman, Stresses due to environmental conditioning of cross-ply graphite/epoxy laminates, in: *Proc. ICCM3*, CD Rom (1980).
12. M. W. Hyer, Some observations on the cured shape of thin unsymmetric laminates, *J. Compos. Mater.* **15**, 175–194 (1981).
13. S. R. White and A. B. Hartman, Effect of cure state on stresses relaxation in 3501-6 epoxy resin, *J. Eng. Mater. Technol.* **119**, 262–265 (1997).
14. P. Olivier, Study of residual curing stresses in carbon/epoxy laminates in relation with the polymerization cycles, PhD Report of Université Paul Sabatier (France) (1994).
15. N. Ersoy and Ö. Vardar, Measurement of residual stresses in layered composites by compliance method, *J. Compos. Mater.* **34**, 575–598 (2000).
16. M. P. I. M. Eijpe and P. C. Powell, A modified layer removal analysis for the determination of internal stresses in polymer composites, *J. Therm. Compos. Mater.* **10**, 334–352 (1997).
17. O. Sicot, X. L. Gong, A. Cherouat and J. Lu, Determination of residual stresses in composite laminates using the incremental hole-drilling method, *J. Compos. Mater.* **37**, 831–844 (2003).
18. O. Sicot, X. L. Gong, A. Cherouat and J. Lu, Influence of experimental parameters on determination of residual stresses using the incremental hole-drilling method, *Compos. Sci. Technol.* **64**, 171–180 (2004).
19. M. L. Benzeggagh, Application of the fracture mechanic theory on composite materials. Example of the delamination fracture of a composite laminate, PhD report of UTC (France) (1980).
20. A. Laksimi, M. Cherfaoui, *et al*., Etude par émission acoustique de l'amorçage et de la propagation de l'endommagement dans un composite verre-époxy, in: *Proc. JNC5*, Paris, France (1986).
21. X. L. Gong, A. Laksimi, D. Laï and M. L. Benzeggagh, Damage analysis of glass/epoxy plates under combined tension-torsion loadings, in: *Proc. ICCM 10*, Vancouver, Canada, pp. 351–358 (1995).
22. S. Benmedakhene, M. Kenane and M. L. Benzeggagh, Initiation and growth of delamination in glass/epoxy composites subjected to static and dynamic loading by acoustic emission monitoring, *Compos. Sci. Technol.* **59**, 201–208 (1999).
23. F. Meraghni, S. Benmedakhane and M. L. Benzeggagh, Identification and modeling of damage mechanisms in short glass fibre reinforced polypropylene composite, in: *Proc. ICCM 10*, Vancouver, Canada, pp. 359–366 (1995).
24. S. Barre and M. L. Benzeggagh, On the use of acoustic emission to investigate damage mechanisms in glass fiber-reinforced polypropylene, *Compos. Sci. Technol.* **52**, 369–376 (1994).